

Azimuthal anisotropies and initial-state fluctuations from SPS to LHC energies

Jovan Milosevic on behalf of the CERES/NA45 and CMS Collaboration^{1,*}

¹ Vinca Institute of Nuclear Sciences, M. Petrovica Alasa 12-14, 11001 Belgrade, Serbia

Abstract. The v_3 coefficient, obtained using the PbAu data from the CERES detector at the top SPS energy of $\sqrt{s_{NN}} = 17.3$ GeV, is presented. The v_2 is measured over a p_T range up to 100 GeV/c in PbPb collisions collected with the CMS detector. The $v_2\{2\}$ of charged and strange particles emitted in pp collisions shows a mass ordering effect. The $v_2\{4\}$ and $v_2\{6\}$ are comparable to the $v_2\{2\}$, and thus supports the collective nature of the long-range correlations in high-multiplicity pp collisions at 13 TeV. Principle Component Analysis (PCA) of two-particle harmonics ($V_{n\Delta}$) is studied in PbPb and high-multiplicity pPb collisions at the LHC. The factorization breaking of the $V_{n\Delta}$ can be attributed to the effect of initial-state fluctuations. Using a PCA, the $V_{n\Delta}$ are characterized through the leading and sub-leading modes. The leading modes are essentially equivalent to the $v_n\{2\}$. The sub-leading modes represent the largest sources of factorization breaking.

1 Introduction

One of main features of Quark Gluon Plasma is its hydrodynamic behavior characterized by v_n coefficients extracted using methods like two- and many-particle correlations [1], the scalar product (SP) [2, 3] and the Lee-Yang Zero (LYZ) [4, 5]. The CMS collaboration measured v_2 coefficient in PbPb collisions over a wide p_T range up to 100 GeV/c [6]. This measurement at high- p_T is complementary to the nuclear modification factor (R_{AA}) measurements. The long-range ($|\Delta\eta| > 2$) correlation known as the ridge is observed not only in PbPb collisions [7], but also in high-multiplicity pPb collisions [8] and even in smallest system formed in high-multiplicity pp collisions [9, 10] giving a hint that the ridge could have a hydrodynamic origin. To support it, the correlations among four or more charged particles are studied in pPb collisions at $\sqrt{s_{NN}} = 5.02$ TeV [11] and in pp collisions at $\sqrt{s} = 5, 7$ and 13 TeV [12]. The two-particle correlations between strange (K_S^0 or $\Lambda/\bar{\Lambda}$) and charged particles [13] also revealed similar ridge structures, and the extracted v_2 , scaled to the number of constituent quarks (n_q) shows that hydrodynamic behavior happens on the partonic level. It is shown in [14, 15] that even if the hydrodynamics is the only source of the long-range correlations, the initial-state fluctuations makes the event plane angle, Ψ_n , dependent on both, p_T and η . This leads to factorization breaking of the $V_{n\Delta}$ into a product of single-particle anisotropies v_n [16]. A PCA [17, 18] is applied on $V_{n\Delta}$ coefficients constructed from 2.76 TeV PbPb collisions and 5.02 TeV high-multiplicity pPb collisions [19]. Within the PCA approach, the $V_{n\Delta}$ coefficients are characterized through leading and sub-leading mode terms. The leading modes are essentially equivalent to the v_n harmonics

*e-mail: Jovan.Milosevic@cern.ch

extracted from two-particle correlations. The sub-leading modes represent the largest sources of factorization breaking. In the context of hydrodynamic models, they are a direct consequence of the initial-state fluctuations.

2 Experiment and data used

About 30 M of central PbAu collisions at the top SPS energy were collected. CERES detector worked in 0.5 T magnetic field which enable precise p_T measurement. The η coverage close to mid-rapidity, together with a full azimuthal (ϕ) coverage enables flow study. Negative pions, identified using the differential energy loss dE/dx in the Time Projection Chamber (TPC) are used in this analysis.

The CMS tracker detector is surrounded with a super-conducting solenoid producing 3.8 T magnetic field which enable precise p_T measurements above 0.3 GeV/c [20]. The PbPb and pPb collisions at the LHC energies of $\sqrt{s_{NN}} = 2.76$ TeV and 5.02 TeV with integrated luminosities of $160 \mu\text{b}^{-1}$ and 35nb^{-1} , respectively, were collected. The data sets for pp collisions at $\sqrt{s} = 5, 7$ and 13 TeV have integrated luminosities of 1.0, 6.2 and 0.7pb^{-1} respectively. A wide pseudorapidity coverage of $|\eta| < 2.5$ for the tracker and $2.9 < |\eta| < 5.2$ for the hadronic forward (HF) calorimeters together with a full azimuthal coverage excellently suites for studying the long-range flow correlations.

3 Results

In figure 1, the comparison between the hydro+UrQMD [21] model predictions and CERES $v_3(p_T)$ measurement of negative pions in PbAu collisions at $\sqrt{s_{NN}} = 17.3$ GeV [22] is shown. The predictions of this model are in a good agreement with the experimental results, except in the p_T region between 0.3 and 0.6 GeV/c where the model slightly underpredicts the experimental data. The $v_3(p_T)$ at the top SPS energy reach only about one half of the corresponding values at the top RHIC and LHC energies. The p_T integrated v_3 value is in an excellent agreement with the STAR v_3 value measured at 19.6 GeV [23]. Within the analyzed range, the CERES v_3 does not show centrality dependence [22].

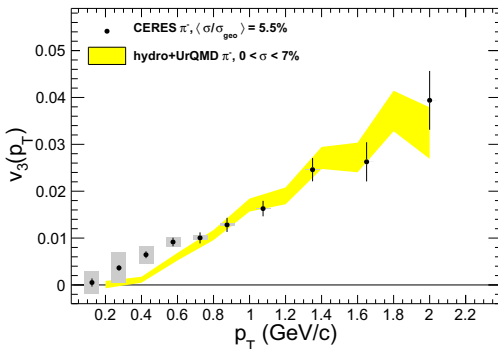


Figure 1. The negative pion $v_3(p_T)$ measured in PbAu collisions at $\sqrt{s_{NN}} = 17.3$ GeV compared with hydro+UrQMD model predictions [22]. Statistical uncertainties are represented with the error bars, while systematic ones are indicated by gray rectangles. Statistical errors of the model predictions are shown as yellow band.

The CMS showed in [6] that the v_3 is consistent with zero while the positive v_2 persists up to very high- p_T of nearly 100 GeV/c. To further explore the nature of the $v_2(p_T)$ dependence, the v_2 values are also calculated using the 4-, 6- and 8- particle cumulant analyses. The obtained results are shown in figure 2. In the low- p_T regions, the results show the usual hydrodynamic shape with $v_2\{\text{SP}\} > v_2\{4\} \approx v_2\{6\} \approx v_2\{8\}$. At high- p_T , results tend to converge to a unique distribution. Such observed collectivity at high- p_T is likely to be related to the jet quenching phenomena and the path-length dependence of the parton energy loss.

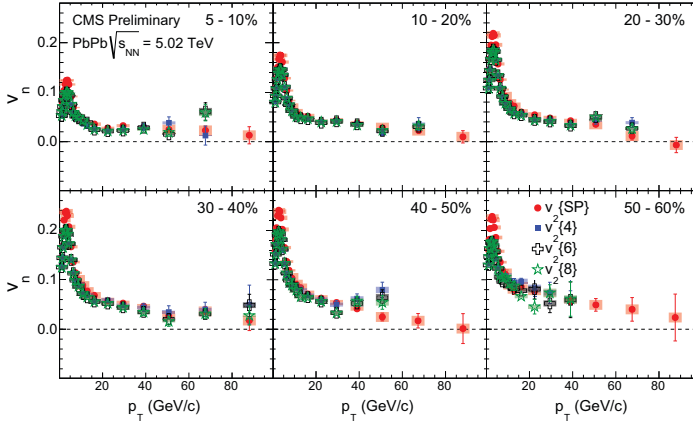


Figure 2. The SP v_2 results compared to those from cumulant method as a function of p_T over wide centrality range in 5.02 TeV PbPb collisions [6]. The systematic uncertainties are denoted with shaded boxes.

The v_2 coefficient in pp collisions at 13 TeV is studied using the two-particle correlation method as well as cumulant of fourth and sixth order [12]. The v_2 , as a function of charged particle multiplicity, are shown in the left panel of figure 3. In the high multiplicity region, the results are consistent with each other. Also, the ordering of the pp results obtained from different methods is similar to what was observed in pPb (middle panel) and PbPb (right panel) collisions [11]: the relation $v_2\{2\} \geq v_2\{4\} \approx v_2\{6\}$ in all three colliding systems is an evidence of a collective behavior.

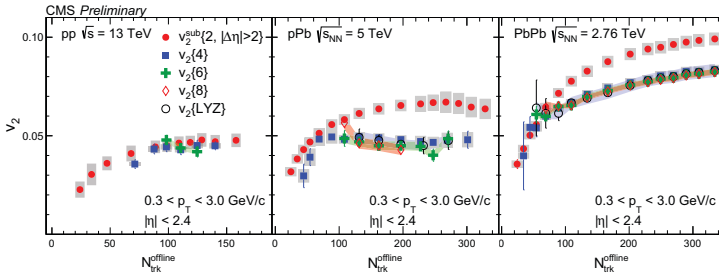


Figure 3. Left: The $v_2\{2\}$, $v_2\{4\}$ and $v_2\{6\}$ vs $N_{\text{trk}}^{\text{offline}}$ for charged particles at 13 TeV pp collisions [12]. Middle (right): The $v_2\{2\}$, $v_2\{4\}$, $v_2\{6\}$, $v_2\{8\}$, and $v_2\{\text{LYZ}\}$ at 5 TeV pPb (2.76 TeV PbPb) collisions [11]. The statistical (systematic) uncertainties are denoted with the error bars (shaded areas).

In order to further investigate possible collective behavior in pp collisions, the v_2 coefficients are also extracted from the correlations between the strange, K_S^0 and $\Lambda/\bar{\Lambda}$, and charged hadrons. The upper panel of figure 4 shows the v_2 values of charged hadrons, K_S^0 mesons and $\Lambda/\bar{\Lambda}$ hyperons as a function of p_T . At small- p_T , a mass ordering in the v_2 is seen in pp collisions. In the bottom panel of figure 4 are presented v_2 values scaled to the number of constituent quarks, n_q , plotted vs scaled kinetic transverse energy, KE_T/n_q , which shows that similarly as in the case of PbPb and pPb [13] collisions, a collective behavior on partonic level is present also in pp collisions at 13 TeV [12].

Due to the initial-state fluctuations, the factorization of the $V_{n\Delta}$ into a product of single-particle anisotropies does not hold precisely. A new observable, r_n (more details in [14–16]) is introduced. It is defined as $r_n = \frac{V_{n\Delta}(p_T^a, p_T^b)}{\sqrt{V_{n\Delta}(p_T^a, p_T^a)} \sqrt{V_{n\Delta}(p_T^b, p_T^b)}}$ which is approximately equal to the $\cos[n(\Psi_n(p_T^a) - \Psi_n(p_T^b))]$. If the r_n is smaller (equal) than 1 then factorization breaks (holds). The value greater than 1 means that there are unremoved non-flow effects. In figure 5 are shown magnitudes of the factorization breaking effect over a wide centrality/multiplicity range. In the case of the 2nd harmonic, the smallest effect is observed for semi-central collisions. Going to more central or more peripheral collisions the size of

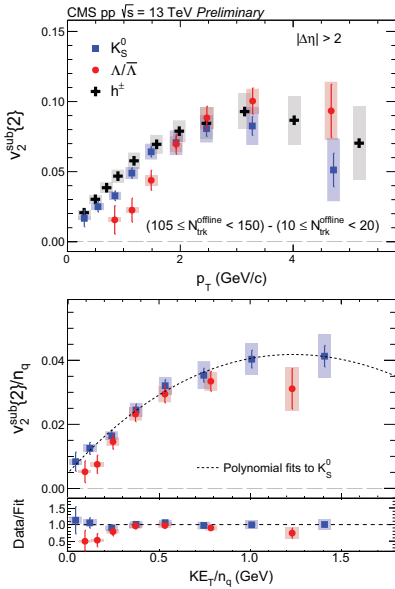


Figure 4. Top: the $v_2(p_T)$ for K_S^0 (blue squares), $\Lambda/\bar{\Lambda}$ (red circles), and charged particles (black crosses) for the multiplicity range $105 \leq N_{\text{trk}}^{\text{offline}} < 150$ in 13 TeV pp collisions. Middle: the n_q -scaled v_2 values of K_S^0 and $\Lambda/\bar{\Lambda}$ particles as a function of KE_T/n_q . Bottom: Ratios of v_2/n_q to a smooth fit of v_2/n_q for K_S^0 vs KE_T/n_q [12]. The error bars correspond to statistical, while the shaded areas to systematic uncertainties.

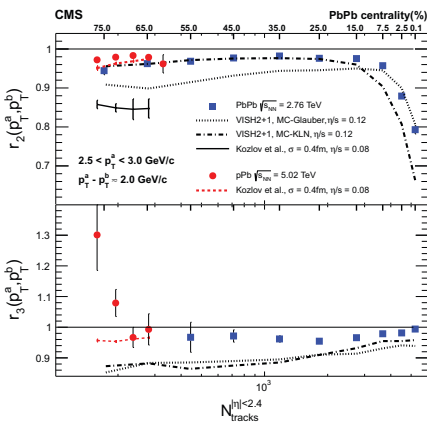


Figure 5. The factorization ratios, r_2 and r_3 , as a function of event multiplicity in pPb and PbPb collisions [16]. The curves show few theoretical predictions for PbPb and pPb collisions. The horizontal solid lines denote the r_2 (top) and r_3 (bottom) value of unity. The error bars correspond to statistical uncertainties, while systematic uncertainties are negligible, and thus are not shown.

the effect increases. At the same multiplicity, the size of the effect is rather similar in the two colliding systems. In PbPb collisions, the size of the r_3 is small and nearly independent of centrality, while in pPb collisions the r_3 approaches to 1 and then goes significantly above 1 at lower multiplicities. The p_T -dependent data are qualitatively described by viscous hydrodynamic models with fluctuating initial-state conditions, while they are insensitive to the shear viscosity to entropy density ratio [16]. This promises of using the factorization data to disentangle contributions of the initial-state conditions and the medium's transport properties to the collective flow, and improving modeling of the evolution of the strongly-coupled quark gluon medium.

The PCA results from 5.02 TeV high-multiplicity pPb and 2.76 TeV PbPb collisions [19] are presented in figure 6 and 7 respectively. The extracted leading flow modes are essentially equal to the results [7, 24] obtained from two-particle correlations. A qualitatively new result obtained using the PCA method is the existence of the sub-leading mode, $v_n^{(2)}$, which is a consequence of the initial-state fluctuations. A non-zero $v_2^{(2)}$ is found both in pPb (left panel in figure 6) and in PbPb (upper

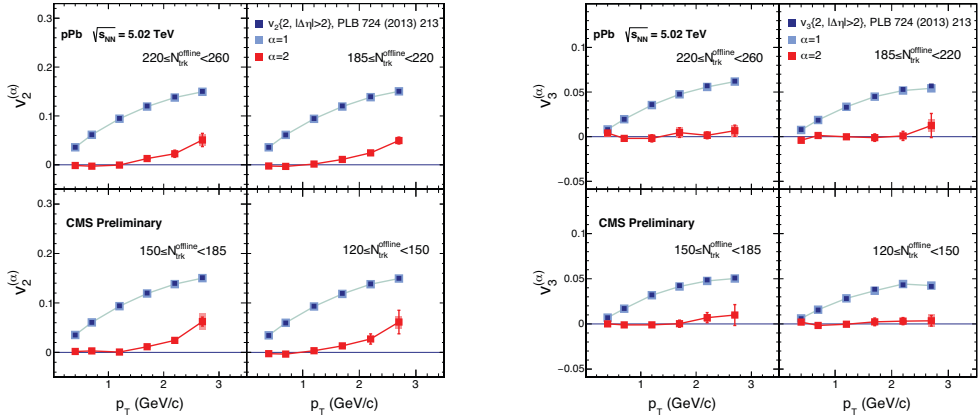


Figure 6. The first and the second mode of $v_2(p_T)$ (left) and $v_3(p_T)$ (right) from 5.02 TeV high-multiplicity pPb collisions [19]. The $v_2^{(1)}$ are compared to the v_n harmonics measured by the CMS collaboration using the two-particle correlation method [7]. The error bars correspond to statistical while shaded areas to systematic uncertainties.

row in figure 7) collisions. It is close to zero at small- p_T and achieves few percent at $p_T \approx 3$ GeV/c. While the strength of the effect does not depend on multiplicity in pPb collisions, there is a centrality dependence of the $v_2^{(2)}$ in PbPb collisions. The similar behavior is established in [16]. The $v_3^{(2)}$ is close to zero in both collision cases (right and bottom panel in figure 6 and 7) which is in an agreement with the results from [16].

4 Summary

In this contribution are presented results on the v_2 and v_3 measurements from the CERES at the top SPS energy, and from the CMS collaboration at the LHC energy. The CMS measured the v_2 up to 100 GeV/c. This result is complementary to the R_{AA} measurements. For the first time, the v_2 has been measured in pp collision at 13 TeV. This, together with the established n_q -scaling shows that collective behavior appears even in such small system as created in pp collision. Also, for the first time sub-leading flow modes, $v_n^{(2)}$, are measured in PbPb and high-multiplicity pPb collisions. The obtained results are in a qualitative agreement with factorization-breaking results.

References

- [1] N. Borghini, P. M. Dinh, and J.-Y. Ollitrault, Phys. Rev C **64**, 054901 (2001)
- [2] C. Adler et al., STAR Collaboration, Phys. Rev. C **66**, 034904 (2002)
- [3] M. Luzum and J.-Y. Ollitrault, Phys. Rev. C **87**, 044907 (2013)
- [4] R. S. Bhalerao, N. Borghini, and J.-Y. Ollitrault, Nucl. Phys. A **727**, 373 (2003)
- [5] N. Borghini, R. S. Bhalerao, and J.-Y. Ollitrault, J. Phys. G **30**, S1213 (2004)
- [6] CMS Collaboration, CMS-HIN-15-014 (2015)
- [7] CMS Collaboration, Phys. Lett. B **724**, 213 (2013)

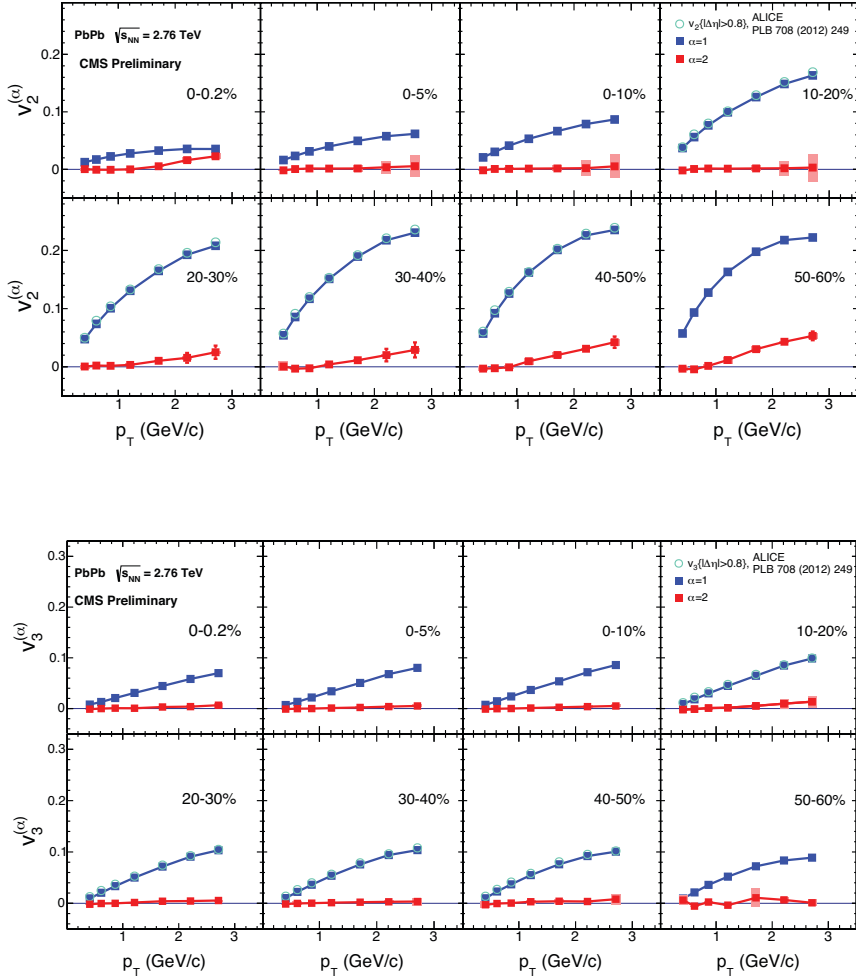


Figure 7. The first and the second mode of $v_2(p_T)$ (upper row) and $v_3(p_T)$ (bottom row) from 2.76 TeV PbPb collisions [19]. The $v_2^{(1)}$ are compared to the v_n harmonics measured by the ALICE collaboration using the two-particle correlation method [24]. The error bars correspond to statistical while shaded areas to systematic uncertainties.

- [8] CMS Collaboration, Phys. Lett. B **718**, 795 (2013)
- [9] CMS Collaboration, JHEP **09**, 091 (2010)
- [10] CMS Collaboration, Phys. Rev. Lett. **116**, 172301 (2016)
- [11] CMS Collaboration, Phys. Rev. Lett. **115**, 012301 (2015)
- [12] CMS Collaboration, arXiv:1606.06198, CMS-HIN-16-010 (2016)
- [13] CMS Collaboration, Phys. Lett. B **742**, 200 (2015)
- [14] F. G. Gardim et al., Phys. Rev. C **87**, 031901 (2013)
- [15] U. Heinz et al., Phys. Rev. C **87**, 034913 (2013)
- [16] CMS Collaboration, Phys. Rev. C **92**, 034911 (2015)

- [17] R. S. Bhalerao, J.-Y. Ollitrault, S. Pal, and D. Teaney, *Phys. Rev. Lett.* **114**, 152301 (2015)
- [18] A. Mazeliauskas, and D. Teaney, *Phys. Rev. C* **91**, 044902 (2015)
- [19] CMS Collaboration, arXiv:1510.03373, CMS-HIN-15-010 (2015)
- [20] CMS Collaboration, *JINST* **3**, S08004 (2008)
- [21] I.A. Karpenko, P. Huovinen, H. Petersen, and M. Bleicher, *Phys. Rev. C* **91**, 064901 (2015)
- [22] D. Adamova et al., CERES NA45 Collaboration, *Nucl. Phys. A* **957**, 99 (2017)
- [23] L. Adamczyk et al., STAR Collaboration, *Phys. Rev. Lett.* **116**, 112302 (2016)
- [24] ALICE Collaboration, *Phys. Lett. B* **708**, 249 (2012)